

Towards equilibration and thermalization between finite quantum systems: The role of dephasing effects and inelastic interactions

Manas Kulkarni^{1,2}, Kunal L. Tiwari^{1,2}, Dvira Segal¹

¹*Chemical Physics Theory Group, Department of Chemistry, University of Toronto, 80 Saint George St. Toronto, Ontario, Canada M5S 3H6 and*

²*Department of Physics, University of Toronto, 60 Saint George St. Toronto, Ontario, Canada M5S 1A7*

(Dated: February 20, 2022)

We demonstrate the approach towards a Gibbs-like equilibrium state, with a common temperature and a chemical potential, of two finite metallic grains, prepared with a different number of noninteracting electrons, connected by a weak link that is susceptible to incoherent and inelastic processes. By developing an analytic method and by using an exact numerical approach, the quantum time evolution of the electrons in the metallic grains is followed. In the absence of decohering and inelastic effects, equilibration is never reached. Introducing dephasing effects on the link *only*, using a dephasing probe, the two quantum systems equilibrate, but do not evolve towards a Gibbs-like state. In contrast, by mimicking inelastic interactions with a voltage probe, the metal pieces evolve towards a common Gibbs-like equilibrium state, with the probe.

PACS numbers: 05.30.-d, 03.65.Aa, 03.65.Yz, 72.10.-d

Introduction. How do quantum systems equilibrate from a certain non-equilibrium initial condition, e.g., a quench [1]? With cold atoms in optical lattices offering a clean experimental setup [2], renewed attention in this fundamental topic has recently sparked. One could address this question with (at least) three distinct setups in mind: (i) Consider an *isolated* quantum system, and study its evolution towards equilibrium, for example, in the time averaged sense [3, 4]. (ii) Attach a subsystem with a few degrees freedom to a thermal reservoir, and monitor the system equilibration, e.g., in the sense of the small trace distance [5, 6], or (iii) put in contact two identical *finite* quantum systems and watch for the process of mutual equilibration [7]. Despite intense efforts, general results are still missing [8]. Recent studies also argue about the precise definition of quantum integrability, and its implication on quantum thermalization [9, 10].

In this work, we consider a combined setup and demonstrate the process of mutual equilibration of two finite metallic quantum systems, connected by a weak link, in the presence of either elastic-decohering processes or inelastic effects, through the interaction of the link electrons with additional degrees of freedom. When only decoherence effects are allowed, the system approaches a non-canonical equilibrium state. In contrast, when inelastic processes are included, the two parts relax towards a common Gibbs-like state. The origin of inelastic scattering processes are many-body interactions in the system, e.g., coupling electrons to phonons. Since an explicit and exact inclusion of such effects is challenging [11–14], it was suggested [15, 16] to phenomenologically introduce elastic and inelastic scattering processes by using dephasing or voltage probes, respectively. These electron reservoirs are prepared such that there is no net (energy resolved or total) electron flow from the system towards these probes.

As a particular realization, we consider the non-

interacting Anderson model with a single electronic level (dot) coupled to two metallic grains (henceforth referred to as reservoirs) [17]. Each reservoir is initially prepared in a distinct Gibbs-like grand canonical state, at a different chemical potential. We follow the time evolution of the reservoirs' electrons, once put in contact through the dot, itself susceptible to decohering and/or inelastic processes. For a schematic representation, see Fig 1. We refer to the metal grains, including (each) $N \sim 500$ electronic states and $n \sim 200$ electrons as “reservoirs”, to indicate that they have a dense-enough density of states, such that their effect on the impurity (dot) can be absorbed into a positive real self-energy function, allowing for a quantum Langevin equation (QLE) description [18]. While we may consider large reservoirs, the number of electrons in the metal grains-dot unit is fixed. However, energy is conserved only in the elastic scattering scenario.

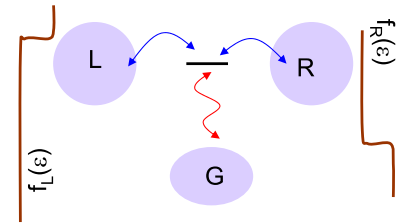


FIG. 1: Two metallic grains (reservoirs) separately prepared in a grand canonical - diagonal state; the initial population is plotted at the boundaries. At t_0 the reservoirs are put into contact through a single electronic state, susceptible to decohering and relaxation effects. This is accounted for by the G reservoir, serving as a dephasing or a voltage probe.

Model. We consider two electron reservoirs $\nu = L, R$, with identical density of states and a sharp cutoff at $\pm D$, which do not directly couple, only through their weak hybridization with a single-state quantum dot. The Hamil-

tonian takes the form

$$H_0 = H_L + H_R + H_W + V_L + V_R, \quad (1)$$

where $H_{L,R,W}$ represents the Hamiltonian for left reservoir, right reservoir and dot, respectively. The term V_ν denotes the coupling of the dot to the ν reservoir,

$$\begin{aligned} H_L &= \sum_l \epsilon_l c_l^\dagger c_l, \quad H_R = \sum_r \epsilon_r c_r^\dagger c_r, \quad H_W = \epsilon_d c_d^\dagger c_d \\ V_L &= \sum_l v_l c_d^\dagger c_l + h.c., \quad V_R = \sum_r v_r c_d^\dagger c_r + h.c. \end{aligned} \quad (2)$$

Here, c_k^\dagger (c_k) are fermionic creation (annihilation) operators of the left reservoir, $l \in L$, right reservoir, $r \in R$ or the dot (d). We assume that v_l and v_r are real numbers and that the Hamiltonians of the metal grains are diagonal in momentum basis. A factorized initial state is assumed, with an empty dot and the reservoirs prepared in a diagonal (grand canonical) state at a chemical potential μ_ν and inverse temperature $\beta = 1/T$, satisfying the distribution $f_\nu(\epsilon) = [e^{\beta(\epsilon - \mu_\nu)} + 1]^{-1}$, $\mu_L = -\mu_R$.

At t_0 the two reservoirs are put into contact through the dot, and their dynamics is followed using either an exact quantum evolution scheme, or a QLE approach (details below). The observed population dynamics is depicted in Fig. 2(a). When the dot level is placed within the bias window, a resonance pattern shows around ϵ_d with a peak developing in the accepting R reservoir and a corresponding dip showing at the L side. The dynamics shown in Fig. 2(a) is fully coherent. Results presented are before the recurrence time $\tau_{rec}^0 \sim 2\pi/\Delta E$; $\Delta E = 2D/N$ is the mean spacing between energy levels [8]. At this time, a complete depletion of certain levels occurs, and the dynamics is reversed.

We now wish to allow for elastic dephasing effects or inelastic interactions on the dot *only*. We mimic such effects with ‘‘probes’’, by augmenting the Hamiltonian (2) by an additional (finite size) electron reservoir G ,

$$H = H_0 + H_G + V_G. \quad (3)$$

Here $H_G = \sum_g \epsilon_g c_g^\dagger c_g$ and $V_G = \sum_g v_g c_d^\dagger c_g + h.c.$. Inelastic effects are introduced using a voltage probe [15, 16], demanding that the net current from the dot to the G unit vanishes, $i_G = 0$. This condition sets an effective chemical potential for this reservoir. Alternatively, elastic dephasing effects can be introduced using a dephasing probe, requiring that $i_G(\epsilon) = 0$, i.e., the charge current at a given energy should vanish. Results are displayed in Fig. 2(b) and (c): The system approaches equilibrium (dephasing probe), and even thermal equilibrium (voltage probe). These results are discussed in details below Eq. (10). We now explain how we time-evolved the system’s density matrix under H_0 or H .

QLE Method. We aim at calculating the time evolution of *all* two-body operators in the system. We begin with the trivial part, the impurity (dot). Since it is coupled to many degrees of freedom, its dynamics can be

described using a quantum Langevin equation [18–21]. We review the steps involved, so as to highlight the underlying approximations, setting the limit for the method applicability. We outline the derivation in the absence of the G probe; We generalize it later to include such a device. In the Heisenberg representation the operators satisfy the following equations of motion (EOM),

$$\begin{aligned} \dot{c}_d &= -i\epsilon_d c_d - i \sum_l v_l c_l - i \sum_r v_r c_r \\ \dot{c}_l &= -i\epsilon_l c_l - i v_l c_d, \quad \dot{c}_r = -i\epsilon_r c_r - i v_r c_d. \end{aligned} \quad (4)$$

Using a formal integration, the l operators follow

$$c_l(t) = e^{-i\epsilon_l(t-t_0)} c_l(t_0) - i v_l \int_{t_0}^t d\tau e^{-i\epsilon_l(t-\tau)} c_d(\tau) d\tau. \quad (5)$$

Similar relations hold for the R operators. We plug these expressions into the dot EOM and get the exact result

$$\begin{aligned} \dot{c}_d &= -i\epsilon_d c_d - \int_{t_0}^t d\tau \sum_l v_l^2 e^{-i\epsilon_l(t-\tau)} c_d(\tau) \\ &\quad - \int_{t_0}^t d\tau \sum_r v_r^2 e^{-i\epsilon_r(t-\tau)} c_d(\tau) - i\eta^L(t) - i\eta^R(t). \end{aligned} \quad (6)$$

Here, $\eta^L(t) \equiv \sum_l v_l e^{-i\epsilon_l(t-t_0)} c_l(t_0)$, and similarly η^R , represent ‘‘noise’’. We now assume that the second and third terms reduce, each, into a dissipation term, further inducing an energy shift of the dot energy, absorbed into the definition of ϵ_d . This is justified here as the metal grains play the role of charge and energy baths with respect to the dot. Under the markovian approximation, we reach the (time local) QLE

$$\dot{c}_d = -i\epsilon_d c_d - i\eta^L(t) - i\eta^R(t) - \Gamma(\epsilon_d) c_d, \quad (7)$$

with $\Gamma(\epsilon) = \sum_{\nu=L,R} \Gamma_\nu(\epsilon)$ and e.g., $\Gamma_L(\epsilon) = \pi \sum_l v_l^2 \delta(\epsilon - \epsilon_l)$. Equation (7) thus relies on two assumptions: (i) a positive real self-energy function $\Gamma_\nu(\epsilon)$ can be written [18], and (ii) the dot dynamics is slow relative to the reservoirs’ evolution. We now use the exact equation (5) and the reduced result (7), and derive analytic expressions for the expectation values $\langle c_k^\dagger(t) c_j(t) \rangle \equiv \text{Tr}[\rho(t_0) c_k^\dagger(t) c_j(t)]$; $k, j = l, r, d$. Here $\rho(t_0) = \rho_d \otimes \rho_L \otimes \rho_R$ is the factorized time-zero density matrix of the system. The trace is performed over all degrees of freedom. In particular, the following initial condition is assumed

$$\begin{aligned} \langle c_d^\dagger(t_0) c_d(t_0) \rangle &= 0, \quad \langle c_l^\dagger(t_0) c_l(t_0) \rangle = f_L(\epsilon_l) \equiv f_l, \\ \langle c_r^\dagger(t_0) c_r(t_0) \rangle &= f_R(\epsilon_r) \equiv f_r. \end{aligned} \quad (8)$$

with $f_\nu(\epsilon) = [e^{\beta(\epsilon - \mu_\nu)} + 1]^{-1}$. The resolved occupation of the, e.g., L reservoir, is given by three contributions,

$$\begin{aligned} p(\epsilon_l) &\equiv \langle c_l^\dagger(t) c_l(t) \rangle = \langle c_l^\dagger(t_0) c_l(t_0) \rangle \\ &\quad + i v_l e^{-i\epsilon_l(t-t_0)} \int_{t_0}^t e^{i\epsilon_l(t-\tau)} \langle c_d^\dagger(\tau) c_l(t_0) \rangle d\tau + c.c. \\ &\quad + v_l^2 \int_{t_0}^t \int_{t_0}^t d\tau_1 d\tau_2 \langle c_d^\dagger(\tau_1) c_d(\tau_2) \rangle e^{i\epsilon_l(t-\tau_1)} e^{-i\epsilon_l(t-\tau_2)}. \end{aligned}$$

The first term accommodates the initial condition. The second element (denoted by F_2) represents first order reservoir-dot coupling processes. The last term (F_3)

corroborates higher order effects, including population transfer from the r reservoir,

$$\begin{aligned}
 F_2 &= -v_l^2 f_l \times (t - t_0) \frac{2\Gamma}{\Gamma^2 + \epsilon_{dl}^2} - 2v_l^2 f_l \frac{\epsilon_{dl}^2 - \Gamma^2}{[\epsilon_{dl}^2 + \Gamma^2]^2} + \frac{v_l^2 f_l e^{-\Gamma(t-t_0)}}{[\epsilon_{dl}^2 + \Gamma^2]^2} \left\{ 2 [\epsilon_{dl}^2 - \Gamma^2] \cos [\epsilon_{dl}(t - t_0)] + 4\epsilon_{dl}\Gamma \sin [\epsilon_{dl}(t - t_0)] \right\} \\
 F_3 &= v_l^2 \sum_{k' \in L, R} \frac{v_{k'}^2 f_{k'}}{\Gamma^2 + \epsilon_{dk'}^2} \left\{ \frac{4 \sin^2 \left[\frac{\epsilon_{lk'}}{2}(t - t_0) \right]}{\epsilon_{lk'}^2} + \frac{1}{\Gamma^2 + \epsilon_{dl}^2} \left[e^{-2\Gamma(t-t_0)} + 1 - e^{(t-t_0)(i\epsilon_{dl}-\Gamma)} - e^{-(t-t_0)(i\epsilon_{dl}+\Gamma)} \right] \right. \\
 &\quad \left. + \left[\frac{1 - e^{-(t-t_0)(\Gamma+i\epsilon_{dl})} + e^{-(t-t_0)(\Gamma+i\epsilon_{dk'})} - e^{-i(t-t_0)\epsilon_{lk'}}}{(\epsilon_{dl} - i\Gamma) \epsilon_{lk'}} + c.c. \right] \right\}. \tag{9}
 \end{aligned}$$

Here, $\epsilon_{jk} = \epsilon_j - \epsilon_k$. For simplicity, the energy dependence of the dissipation terms is ignored. We can immediately confirm that $i_\nu(t) = \frac{d}{dt} \sum_{k \in \nu} \langle c_k^\dagger(t) c_k(t) \rangle$ produces the standard expression for the charge current [22]. We have similarly derived closed expressions for *all* density matrix elements, including off-diagonal elements, e.g., $\langle c_l^\dagger(t) c_{l'}(t) \rangle$, ($l \neq l'$). These lengthy expressions are not presented here. Since the reservoirs include many states, after a short time τ_t , $\Gamma\tau_t \gtrsim 2$, the dot dynamics should remain fixed at a quasi steady-state value, up to the recurrence time τ_{rec}^0 . The interval $\tau_t < t < \tau_{rec}^0$ is identified as the quasi steady-state (QSS) region

We now incorporate the G reservoir, the probe, into this QLE description: The dot dynamics follows Eq. (7) with an additional noise term η^G , and we re-define the total hybridization, $\Gamma = \Gamma_L + \Gamma_R + \Gamma_G$, $\Gamma_G(\epsilon) = \pi \sum_g v_g^2 \delta(\epsilon - \epsilon_g)$. As a result, all expectation values follow a form technically identical to the $\Gamma_G = 0$ limit. For example, the population $\langle c_l^\dagger(t) c_l(t) \rangle$ obeys Eq. (9), augmented by $k' \in G$ terms in F_3 . To include *inelastic scattering effects* of electrons on the dot, we implement a voltage probe assuming $f_G(\epsilon) = [e^{\beta(\epsilon - \mu_G)} + 1]^{-1}$. The chemical potential μ_G is set such that $i_G \equiv \frac{d}{dt} \sum_g \langle c_g^\dagger c_g \rangle = 0$ is satisfied at all simulation time. With the motivation to explore situations beyond the linear response regime [20], we retrieve μ_G numerically, by employing the Newton-Raphson method [23], $\mu_G^{(k+1)} = \mu_G^{(k)} - i_G(\mu_G^{(k)})/i'_G(\mu_G^{(k)})$. $\mu_G^{(0)}$ is the initial guess, i'_G is the first derivative with respect to μ_G . In principle, one should adjust μ_G throughout the simulation, to eliminate population leakage from the L -dot- R system. However, we have practically found that within the allowed simulation time (details below) we could safely assume a QSS limit. The energy resolved charge current into G can then be written as

$$i_G(\epsilon) = \frac{2\Gamma_G}{\pi} \frac{\Gamma_R[f_G(\epsilon) - f_R(\epsilon)] + \Gamma_L[f_G(\epsilon) - f_L(\epsilon)]}{(\epsilon - \epsilon_d)^2 + \Gamma^2},$$

with the total current $i_G = \int i_G(\epsilon) d\epsilon$. *Quasi-elastic scattering* effects are implemented within a dephasing

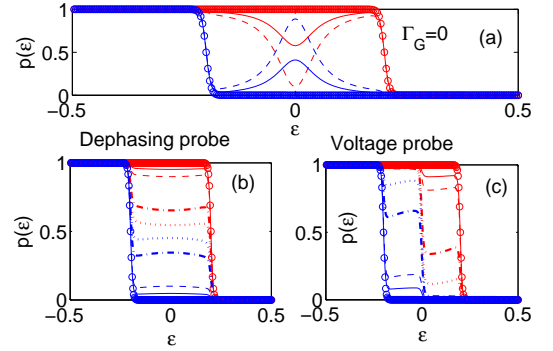


FIG. 2: (a) Coherent population dynamics of the reservoirs' electrons. Plotted are the L (three top lines) and R (three bottom lines) occupations as a function of electron energy, for $\Gamma_G = 0$ at $t = 0$ (\circ) $t = 750$ (full) and $t = 1500$ (dashed). (b) Approaching a non-canonical equilibrium state with a dephasing probe, L -bath (five top lines) and R -bath (five bottom lines) occupation functions. (c) Approaching thermal equilibrium with a voltage probe, L -bath (five right-most lines) and R -bath (five left-most lines) occupation functions. In (b) and (c) $\Gamma_G = 0.4$ and $t = 0$ (\circ), $t = 750$ (full), $t = 1500$ (dashed), $t = 7500$ (dashed-dotted) and $t = 15 \times 10^3$ (dotted). The last two lines were generated by restarting the QLE dynamics when approaching $t = m\tau_{rec}^0$, m is an integer. μ_G has been further updated at each restart point to eliminate leakage. In all panels $\beta = 200$, $\Gamma_L = \Gamma_R = 0.025$. $\epsilon_d = 0$, $\mu_L = -\mu_R = 0.2$, $D = 1$, $N = 500$ electronic states at each reservoir, L, R, G .

probe, by demanding that $i_G(\epsilon) = 0$, to yield $f_G(\epsilon) = \frac{\Gamma_R f_R(\epsilon) + \Gamma_L f_L(\epsilon)}{\Gamma_R + \Gamma_L}$.

Exact method. Even with the inclusion of the probe, the QLE description is still technically limited by the recurrence time $t < \tau_{rec}^0 \propto N_{L,R}$ ($N_{L,R}$ is the number of electronic states in a *single* metallic grain), though no actual population recurrence does show in the dynamics. This is because the validity of Eq. (7) is limited by this time, beyond which inter-reservoir recurrences, that may not show in the overall behavior, take place. Us-

ing an *exact*, expensive, brute force calculation, we can numerically simulate ($A \equiv c_j^\dagger c_k$)

$$\begin{aligned} \langle A(t) \rangle &= \text{Tr}_B[\rho(t_0)e^{iHt} A e^{-iHt}] \\ &= \lim_{\lambda \rightarrow 0} \frac{\partial}{\partial \lambda} \text{Tr}_B[\rho_L \rho_R \rho_G \rho_d e^{iHt} e^{\lambda A} e^{-iHt}], \end{aligned} \quad (10)$$

using the fermionic trace formula [24]. Here, $\rho_\nu = e^{-\beta(H_\nu - \mu_\nu N_\nu)} / Z_\nu$; Z_ν is the partition function. Such a calculation perfectly agrees with QLE results, further confirming that beyond τ_{rec}^0 , where QLE description breaks down, the dynamics proceed towards equilibrium, before $\tau_{rec} \propto \sum_{i=L,R,G} N_i$, see Fig. 3. We now show an approach towards equilibrium within $t < \tau_{rec}$ using the exact method, and $t < \tau_{rec}^0$ using the QLE technique.

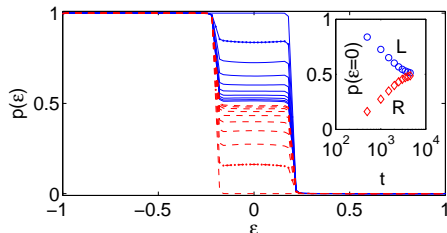


FIG. 3: Equilibration with a dephasing probe, using an exact-unitary time evolution scheme, Eq. (10). $N_L = N_R = 100$, $N_G = 1500$, other parameters are the same as in Fig. 2(b). The L (full) and R (dashed) populations are shown at $t = 0 : \delta t : 9\delta t$, $\delta t = 500$. The dotted lines mark the values reached before recurrence if $N_G = 200$. The inset demonstrates a slow-down in dynamics in approaching the equilibrium state.

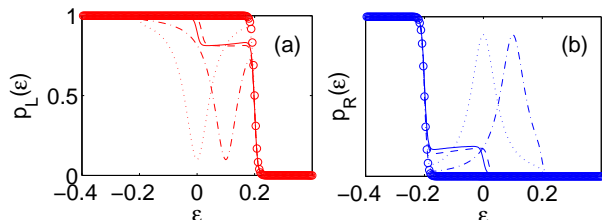


FIG. 4: (a) Occupation of L bath at time $t = 0$ (o) and $t = 1500$ for $\Gamma_G = 0$ and $\epsilon_d = 0$ (dotted), $\Gamma_G = 0$ and $\epsilon_d = 0.1$ (dashed-dotted), $\Gamma_G = 0.4$ and $\epsilon_d = 0$ (full), $\Gamma_G = 0.4$ and $\epsilon_d = 0.1$ (dashed). The latter two lines assume the voltage probe condition. (b) Same for the R side occupations. Other parameters are the same as in Fig. 2(c).

Results. We identify thermal equilibration in our peer-quantum system setup, by adjusting the conditions of Refs. [5, 10], demanding that: (i) The system should equilibrate, i.e., evolve towards some particular state, and stay close to it for almost all time. Furthermore, the equilibrium state should be (ii) independent of the dot properties-energetics and initial state, (iii) insensitive to the precise initial state of each reservoir, (iv) close to diagonal in the energy basis of its eigen-Hamiltonian, and (v) a Gibbs state.

In Fig. 2(b)-(c) we use the QLE method and follow the reservoirs' mutual equilibration process, using either a dephasing probe (b) or a voltage probe (c). We present the reservoirs' occupation at times $t/75 = 0, 10, 20, 100, 200$. Beyond $\tau_{rec}^0 \sim 1500$ the QLE description breaks down; The data at later times has been generated by restarting the simulation immediately before τ_{rec}^0 , using the L and R final diagonal-distribution as an initial condition for a new run, with the G bath re-adjusted to respect the probe condition. This process can be repeated, to reach a complete equilibration. It can be realized experimentally by fine-tweaking the voltage probe (introducing a dissipation mechanism into the dynamics) [25]. When only dephasing effects are allowed, the system is approaching a non-thermal state. Ultimately, the population of the two reservoirs should reach a two-step function with $p(\mu_R < \epsilon < \mu_L) \sim 0.5$, since excess electrons at the L side loose their phase memory, therefore, on average, half of them populate the R side in the long time limit. This equilibrium state is sensitive to the precise details of the initial electron distribution, as energy redistribution is not allowed. In contrast, when inelastic effects are taking place, the system does approach a Gibbs-like thermal state, a step function at zero temperature.

Simulations with a dephasing probe using the exact-unitary method, Eq. (10), up to $\tau_{rec} \propto \sum_{i=L,R,G} N_i$, are shown in Fig. 3, demonstrating a clear evolution towards an equilibrium state. We build a large G so as to delay recurrence. Results at earlier times do not depend on the size of G , reinforcing the observation that G acts as an agent in driving the L - R mutual equilibration process. QLE data with G bath tweaking nicely agrees with these results. In order to show the analogous behavior with a voltage probe, a dissipative mechanism should be introduced into the G bath, e.g., by building a hierarchy of its interactions with the L - R system.

Fig. 4 proves that while under coherent evolution the resonance peak emerges around the energy ϵ_d , in the presence of a voltage probe with (large enough) Γ_G , the buildup of the equilibrium state systematically occurs around the equilibrium Fermi energy, independently of the link energetics. This holds even when the dot is placed *outside* the bias window (not shown). Using a smaller value for Γ_G , temporal features show, washed out gradually in approaching the equilibrium state. Analogous trends also take place when allowing for dephasing only.

The thermal state should be diagonal in the energy eigenbasis of its Hamiltonian [5]. In Fig. 5 we display the density matrix (DM) $\rho_{l,\nu} = \langle c_l^\dagger c_\nu \rangle$, excluding diagonals, with and without a voltage probe, using the QLE technique. This quantity is expected to oscillate in the long time limit since the Hamiltonian is not diagonal in the (local) l basis. We still show the results in this basis, so as to manifest local ν -bath properties. A subtle source of complication is the fact that $\rho_{l,\nu}$ decays (before τ_{rec}^0), even without a probe, due to the finite-bias

assumed as an initial condition. One should therefore differentiate between bias-induced and probe-induced decoherence processes. There are three significant differences in the behavior of off-diagonal elements, with and without the probe: (i) The absolute value of the coherences, at a given time, is smaller when $\Gamma_G \neq 0$. (ii) The DM approaches a diagonal form (strict diagonal values are not shown). (iii) When $\Gamma_G = 0$, oscillations occur around ϵ_d . With the probe, contributions appear mainly around the equilibrium Fermi energy.

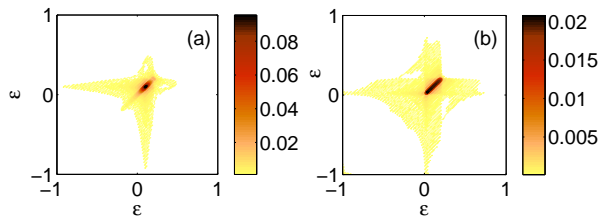


FIG. 5: Absolute values of the density matrix elements $\rho_{l,l'}$ at $t = 1500$ (a) $\Gamma_G = 0$, (b) using a voltage probe, $\Gamma_G = 0.4$. Other parameters are the same as in Fig. 2(c), $\epsilon_d = 0.1$.

Summary. We provided evidence, using analytical and numerical tools, showing that two finite quantum systems, coupled through a weak link where electrons can lose phase memory or exchange energy, can equilibrate

and even thermalize. Dephasing and voltage probes are cunning techniques, allowing to mimic memory loss and energy redistribution. We could follow the time evolution of the peer metals numerically-exactly or using an analytic QLE scheme, where tweaking the probes with a new initial state drives the peer-metal system closer and closer to the equilibrium state. Our results are significant for several reasons: (i) We show that inelastic or dephasing effects on a very small- yet essential- subset of the total system can drive the system towards a global equilibrium state, where thermal equilibration is approached in the former case. (ii) The colloquial, restrictive, “nondegenerate energy gap” condition [3–5, 7] is not assumed in our study. (iii) Standard QLE treatments [18] overlooked reservoirs’ dynamics all-together. Here, we frame a new tool for studying the dynamics of a system composed of many degrees of freedom, by identifying a subsystem and resolving its dynamics, then using this information backward, to re-explore the evolution of all degrees of freedom. Future directions include the study of electron-electron interaction effects [26], and considering a quantum dot chain between the two metal grains. Here, the charge current coherent-diffusive crossover [27] may reflect itself in the energy reorganization of the reservoirs.

This work has been supported by NSERC. M.K. thanks Diptiman Sen for useful discussions.

-
- [1] A. Polkovnikov, K. Sengupta, A. Silva, and M. Vengalattore, *Rev. Mod. Phys.* **83**, 863 (2011).
 - [2] I. Bloch, J. Dalibard, and W. Zwerger, *Rev. Mod. Phys.* **80**, 885 (2008).
 - [3] P. Reimann, *Phys. Rev. Lett.* **101**, 190403 (2008); *New J. Phys.* **12**, 055027 (2010).
 - [4] A. J. Short, *New J. Phys.* **13**, 053009 (2011).
 - [5] N. Linden, S. Popescu, A. J. Short, and A. Winter, *Phys. Rev. E* **79**, 061103 (2009).
 - [6] J. Dajka, J. Luczka, and P. Hänggi, *Phys. Rev. A* **84**, 032120 (2011).
 - [7] A. V. Ponomarev, S. Denisov, and P. Hänggi, *Phys. Rev. Lett.* **106**, 010405 (2011).
 - [8] V. I. Yukalov, *Laser Phys.* **8**, 485 (2011).
 - [9] J.-S. Caux, and J. Mossel, *J. Stat. Mech.: Theory and Exp.* P02023 (2011).
 - [10] C. Gogolin, M. P. Müller, and J. Eisert, *Phys. Rev. Lett.* **106**, 040401 (2011).
 - [11] L. Mühlbacher and E. Rabani, *Phys. Rev. Lett.* **100**, 176403 (2008).
 - [12] H. Wang, I. Pshenichnyuk, R. Härtle and M. Thoss, *J. Chem. Phys.* **135**, 244506 (2011).
 - [13] R. Hütten, S. Weiss, M. Thorwart, and R. Egger, *Phys. Rev. B* **85**, 121408 (2012).
 - [14] Y. Vinkler, A. Schiller, and N. Andrei, *Phys. Rev. B* **85**, 035411 (2012).
 - [15] M. Büttiker, *Phys. Rev. B* **32**, 1846 (1985), *Phys. Rev. B* **33**, 3020 (1986).
 - [16] M. J. M. de Jong and C. W. J. Beenakker, *Physica A* **230**, 219 (1996).
 - [17] P. W. Anderson, *Phys. Rev.* **124**, 41 (1961).
 - [18] G. W. Ford, J. T. Lewis, and R. F. O’Connell, *Phys. Rev. A* **37**, 4419 (1988).
 - [19] A. Dhar and D. Sen, *Phys. Rev. B* **73**, 085119 (2006).
 - [20] D. Roy and A. Dhar, *Phys. Rev. B* **75**, 195110 (2007).
 - [21] A. Dhar, K. Saito, and P. Hänggi, *Phys. Rev. E* **85**, 011126 (2012).
 - [22] T. L. Schmidt, P. Werner, L. Mühlbacher and A. Komnik, *Phys. Rev. B* **78**, 235110 (2008).
 - [23] W. H. Press, B. P. Flannery, S. A. Teukosky, and W. T. Vetterling, *Numerical Recipes in C: The Art of Scientific Computing*, (Cambridge University Press 1992).
 - [24] I. Klich, in “Quantum Noise in Mesoscopic Systems”, edited by Yu. V. Nazarov and Ya. M. Blanter (Kluwer, 2003).
 - [25] P. Roulleau, *et al.*, *Phys. Rev. Lett.* **102**, 236802 (2009).
 - [26] D. Segal, A. J. Millis, and D. R. Reichman, *Phys. Rev. B* **82**, 205323 (2010).
 - [27] F. Bonetto, J. L. Lebowitz, and J. Lukkarinen, *J. Stat. Phys.* **116**, 783 (2004).